University of Wollongong
Research Online

Faculty of Engineering - Papers (Archive)

Faculty of Engineering and Information Sciences

2012

Abnormal magnetic behaviors and large magnetocaloric effect in MnPS3 nanoparticles

R Zeng
University of Wollongong, rzeng@uow.edu.au

S Q. Wang
Hubei University

G D. Du
University Of Wollongong, gd616@uow.edu.au

Jianli Wang
University of Wollongong, jianli@uow.edu.au

J C. Debnath
University Of Wollongong

See next page for additional authors

http://ro.uow.edu.au/engpapers/5047

Publication Details

Zeng, R., Wang, S. Q., Du, G. D., Wang, J. L., Debnath, J. C., Shamba, P., Fang, Z. Y. & Dou, S. X. (2012). Abnormal magnetic behaviors and large magnetocaloric effect in MnPS3 nanoparticles. Journal of Applied Physics, 111 (7), 07E144-1-07E144-3.

Research Online is the open access institutional repository for the University of Wollongong. For further information contact the UOW Library: research-pubs@uow.edu.au

Authors
R Zeng, S Q. Wang, G D. Du, Jianli Wang, J C. Debnath, Precious Shamba, Z Y. Fang, and S. X. Dou

This journal article is available at Research Online: http://ro.uow.edu.au/engpapers/5047

AIP Journal of Applied Physics

Abnormal magnetic behaviors and large magnetocaloric effect in MnPS3 nanoparticles

R. Zeng, S. Q. Wang, G. D. Du, J. L. Wang, J. C. Debnath et al.

Citation: J. Appl. Phys. **111**, 07E144 (2012); doi: 10.1063/1.3679409
View online: http://dx.doi.org/10.1063/1.3679409
View Table of Contents: http://jap.aip.org/resource/1/JAPIAU/v111/i7
Published by the American Institute of Physics.

Related Articles

Magnetization of 2.6T in gadolinium thin films
Appl. Phys. Lett. 101, 142407 (2012)

Amorphous Slater-Pauling like behaviour in magnetic nanoparticles alloys synthesized in liquids
J. Appl. Phys. 112, 063910 (2012)

On the influence of nanometer-thin antiferromagnetic surface layer on ferromagnetic CrO2
J. Appl. Phys. 112, 053921 (2012)

Thermal stability and the magnetic properties of hybrid vanadium oxide-tetradecylamine nanotubes
J. Appl. Phys. 112, 053912 (2012)

Nanostructured thin manganite films in megagauss magnetic field
Appl. Phys. Lett. 101, 092407 (2012)

Additional information on J. Appl. Phys.

Journal Homepage: http://jap.aip.org/
Journal Information: http://jap.aip.org/about/about_the_journal
Top downloads: http://jap.aip.org/features/most_downloaded
Information for Authors: http://jap.aip.org/authors

ADVERTISEMENT

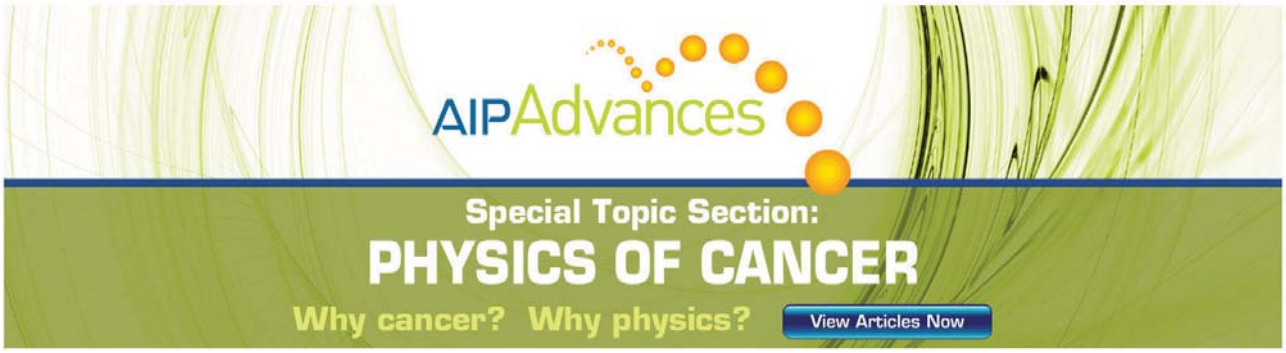

Downloaded 09 Oct 2012 to 130.130.37.84. Redistribution subject to AIP license or copyright; see http://jap.aip.org/about/rights_and_permissions

Abnormal magnetic behaviors and large magnetocaloric effect in $MnPS_3$ nanoparticles

R. Zeng,[1,a)] S. Q. Wang,[2] G. D. Du,[1] J. L. Wang,[1] J. C. Debnath,[1] P. Shamba,[1] Z. Y. Fang,[1] and S. X. Dou[1]
[1]*Institute for Superconducting and Electronic Materials, University of Wollongong, NSW 2522, Australia*
[2]*School of Chemical Engineering, University of Hubei, Wuhan 430036, People's Republic of China*

(Presented 1 November 2011; received 11 October 2011; accepted 7 December 2011; published online 12 March 2012)

A nanostructured honeycomb lattice consisting of $MnPS_3$ nanoparticles synthesized via the ion-exchange technique was found to have restacked molecular layers stabilized by H_2O insertion between the layers. Susceptibility (χ) and heat capacity measurements showed the absence of long range magnetic ordering, at least down to 2 K. However, the χ data showed that the system possesses a high effective Curie temperature, suggesting that the system is in a high spin lattice disordered state. Evaluation of the magnetocaloric effect indicates that the system has a large reversible magnetic-entropy change ($-\Delta S_m$) of 6.8 and 12.8 J/kg K and an adiabatic temperature change (ΔT_{ad}) of 3.8 K and 8 K at 2.85 K for magnetic field changes of 3 T and 9 T, respectively. © *2012 American Institute of Physics*. [doi:10.1063/1.3679409]

MPX_3 (M = Mn, Fe, Co, Ni, etc. transition metals; X = S, Se) compounds have attracted much attention[1–13] to this family due to their layered structure combined with high anisotropy; their special, but still uncertain and interesting, magnetic orderings[1,2]; and their potential applications as cathode material for secondary batteries,[3] ion-exchange applications,[4] ferroelectric materials,[5] and non-linear optically active materials,[6,7] as well as their very interesting potential to yield molecular magnets via the intercalation of exotic polymer layers.[9–12] Bulk $MnPS_3$ is a layered honeycomb lattice quasi-2-dimensional antiferromagnet,[1] and studies of its magnetic properties and neutron spectra have reported powder and crystal materials with a Néel ordering temperature $T_N = 78$ K and a large spin potential ($S = 5/2$) of the Mn ions, but there have been no reports on the magnetic properties and magnetocaloric effect of its special nanostructure form as yet.

A polycrystalline nanoparticle sample of $MnPS_3$ was prepared via the ion-exchange solvothermal method according to the literature.[13]

Figure 1(a) displays the XRD pattern of the $MnPS_3$ nanoparticles. The indexing of diffraction peaks of the $MnPS_3$ nanoparticles is marked, with the lines of the corresponding bulk material standard (JCPDS No. 78-0495) included as well. It should be noted that all diffraction peaks can be indexed to a monoclinic cell with lattice constants $a = 6.077$ Å, $b = 10.524$ Å, $c = 6.769$ Å, and $\beta = 107.35°$, indicating that the crystal structure of the $MnPS_3$ nanoparticles belongs to space group $C2/m$. The peaks of nanoparticles are much broader than those of the bulk materials due to the smaller particle size and the lattice distortion due to the nanosize. Only {001} Bragg peaks are detectable, and the individual peaks show water tails, i.e., Warren tails,[14] suggesting that the system is a monolayer or consists of restacked monolayers with a water stabilized structure. Frindt *et al.* have exfoliated the layered compounds $MnPS_3$ and $CdPS_3$ to form single molecular layers in suspension in water using the same ion exchange method.[14] Our XRD results are the same as in their reports, indicating that our nanoparticles are restacked single molecular layers separated by crystallised H_2O. The H_2O separates the individual molecular layers and stabilizes the restacked structure. The XRD data also show a nearly pure single phase, as there is not an obvious impurity peak in Fig. 1(a). The morphology of the $MnPS_3$ nanoparticles was investigated via SEM, as shown in Fig. 2(b). The $MnPS_3$ is shown to have platelet shaped particles 10 to 20 nm thick with a diameter distribution range of 20 to 50 nm.

The temperature dependence of the susceptibility (χ) under zero field cooling and field cooling in a field H = 100 Oe is plotted in the inset of Fig. 2(a). The temperature dependence of the inverse susceptibility ($1/\chi$) and the Curie constant $C_{CW}(T) \equiv \chi T$ are also shown in Fig. 2(a). There is no sign of any long-range ordering temperature for these $MnPS_3$ nanoparticles from the χ–T, $1/\chi$–T, and χT–T curves.

The $1/\chi$–T curves for temperatures > 150 K have been fitted by using the Curie-Weiss formula ($\chi_C = C_{CW}/(T + \Theta_{CW})$). The fitting and calculation results show unusual features: a very large $C_{CW} = 23.3$ emu/mol, $\mu_{eff} = 13.6\,\mu_B$, and $\Theta_{CW} = -519$ K under field $H = 100$ Oe. Selected inverse susceptibility ($1/\chi$)–T curves under different fields are shown in Fig. 2(a), and the fitting results are plotted in Fig. 2(b).

The fitting and calculations indicate that this system presents unusual electronic and spin features, including a large effective magnetic moment ($\mu_{eff} = 13.6\,\mu_B$) under a field of 100 Oe, which is double the molecular field theoretical Mn^{2+} ion local spin moment $\mu_{eff}^{Th} = [4S(S+1)]^{1/2} = 5.9\,\mu_B$ ($S = 5/2$ for Mn^{2+} ion). However, the effective magnetic moment (μ_{eff}) presents strong field dependence; for example, μ_{eff} decreases from 13.6 μ_B under a field of 100 Oe to 5.9 μ_B under fields >20 kOe, as shown in the inset of Fig. 2(b), which presents the non-linear field-polarization characterization of the 2D electron system.[17] Also,

[a)]Author to whom correspondence should be addressed. Electronic mail: rzeng@uow.edu.au.

 © 2012 American Institute of Physics

Downloaded 09 Oct 2012 to 130.130.37.84. Redistribution subject to AIP license or copyright; see http://jap.aip.org/about/rights_and_permissions

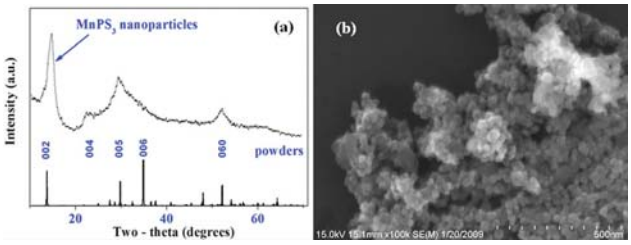

FIG. 1. (Color online) (a) X-ray diffraction pattern with lines from the corresponding bulk standard included and (b) SEM image of the $MnPS_3$ nanoparticles.

$\Theta_{CW} = -519$ K, and the possible long range ordering temperature < 2 K, so the system's frustration factor $f = \Theta_{CW}/T_C\ (T_N) > 259.5$, where a high value of f indicates that the system has fallen into strong disordered electron and spin competing interaction.

Our analysis of χ, the heat capacity (C_P) measurements, and Wilson's ratio (R_W, also known as the Sommerfeld ratio) support the conjecture that the possible spin-liquid-like abnormal spin behavior might emerge from this system. As shown in Fig. 2(a), when the temperature <8 K (100 Oe), χ has a linear relationship with $-\log(T)$, and all straight lines under different applied fields are nearly parallel to each other, with the field only slightly changing the slope of the line. The log-log plots of the C_P/T–T curves under fields from 0 to 9 T are shown in Fig. 2(c), and the semi-log plots are presented in the inset. The curves do not show any anomalous peaks, but they do show a slight upturn in the lower temperature range. These results again indicate the absence of long-range ordering over the entire measured temperature range. The upturn appearing at the lowest temperatures may be attributed to a nuclear Schottky contribution of the Mn cations in the counter-anion, mostly likely the S anions, because the system consists of multi-layered particles by the restacking of monomolecular layers through the insertion of H_2O and the breaking of S-S bonds. The absence of thermal anomalies is consistent with the abovementioned magnetic susceptibility measurements. Considering the upturn in C_P, in order to more accurately evaluate the conduction electron specific heat coefficient γ, we directly fitted the low-temperature C_P data to the formula

$$C_p = A/T^2 + \gamma T + \beta T^3, \tag{1}$$

where the values for the coefficients are $A = 0.25$ mJ K mol^{-1}, $\gamma = 156$ mJ K^{-2} mol^{-1}, and $\beta = 2.3$ mJ K^{-4} mol^{-1} for $H = 0$ T. Similarly, we directly fitted the C_P temperature dependence curves under fields from 0 to 90 kOe, and the results are shown in Fig. 2(d). Wilson's ratio is defined as the dimensionless quantity

$$R_W \equiv 4\pi^2 k_B^2 \chi(0)/3(g\mu_B)^2\gamma, \tag{2}$$

where g is the gyromagnetic ratio in the absence of interactions, k_B Boltzmann's constant, μ_B is the Bohr magneton, and $\chi(0)$ is the residual magnetic susceptibility at temperature $T \to 0$ K, e.g., $\chi(0) = \chi(T \to 0)$. For a non-interacting Fermi gas, $R_W = 1$. Wilson showed that for the Kondo model, the impurity contributions to $\chi(0)$ and γ give a universal value of $R_W = 2$, independent of the strength of the interactions.[18,19] Extrapolation of the linear temperature dependence of the inverse susceptibility down to $T = 0$ K via line fitting simply gives a residual magnetic susceptibility of $1/\chi(0)$. The $\chi(0)$ values are calculated from the above data on $1/\chi(0)$, and the results are shown in Fig. 2(a). The Wilson ratio R_W can be determined according to Eq. (2), and the results are shown in Fig. 2(d). As Fig. 2(d) shows, γ is not seriously affected by magnetic field, but it slightly increases as the field increases up to 3 T, and then it slightly decreases. R_W has its minimum value at the field $H = 3.0$ T, indicating a decreasing electron-electron correlation, because the large temperature independent magnetic susceptibility χ_0 is in the range of the free electron system. These values of R_W (0.6 to 2.16) imply a proper scaling of $\chi(0)$ and suggest that γ exists in the Fermi liquid state.

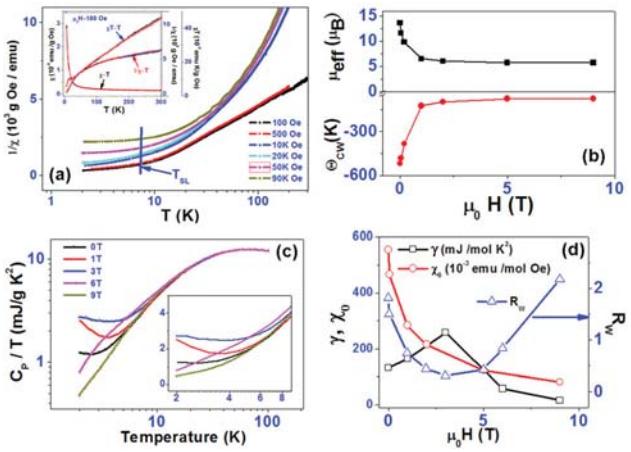

FIG. 2. (Color online) (a) Semi-log plots of $1/\chi$–T curves under the indicated fields; the inset is the temperature dependence of the magnetic susceptibility (χ) and inverse susceptibility ($1/\chi$) under zero field cooling (black symbol line) and field cooling (red symbol line) in an external magnetic field $H = 100$ Oe (χ–T and inverse $1/\chi$–T curve). (b) Susceptibility fitting results at high temperature range ($T > 200$ K). (c) Log-log plots of Cp/T vs T in the low-temperature region under different fields; semi-log plots are included in the insets. (d) $\chi(0) \approx \chi_0$ ($T \to 0$ K), finite electronic heat capacity coefficient γ, and Wilson ratio R_W determined by using low temperature data from 2.1 K to 10 K (see text) as a function of field.

The degeneracy of the energy states of disordered abnormal spins should give rise to gapless excitations or continuously gapped excitations, which are very beneficial for the magnetocaloric effect (MCE) because (i) they make the spins in the system easier to align under external magnetic field, and the low lying energy and even gapless spectrum create a high entropy ground state, and this plus the large spin potential ($S = 5/2$) of the Mn^{2+} ions make it possible to achieve very high MCE; and (ii) the theoretical moment is 5.9 μ_B/f.u. for the $MnPS_3$ system, based on the local magnetic moment model, and the greatest possible magnetic entropy change $-\Delta S_M$ would be $-\Delta S_M = Nk_B \ln(2J+1) \approx 83.15$ J/kg K, where N is the number of spins and J is the quantum number of the spin. The value of $-\Delta S_M$ indicates that the system may achieve a large MCE in the low temperature range.

The isothermal magnetization curves for the $MnPS_3$ nanoparticles in the temperature range between 2.7 and 24 K under fields of up to 9 T are shown in Fig. 3(a). Arrott plot (not shown here) analysis indicated that the system did not have any transitions, only spin fluctuations, which confirmed

Downloaded 09 Oct 2012 to 130.130.37.84. Redistribution subject to AIP license or copyright; see http://jap.aip.org/about/rights_and_permissions

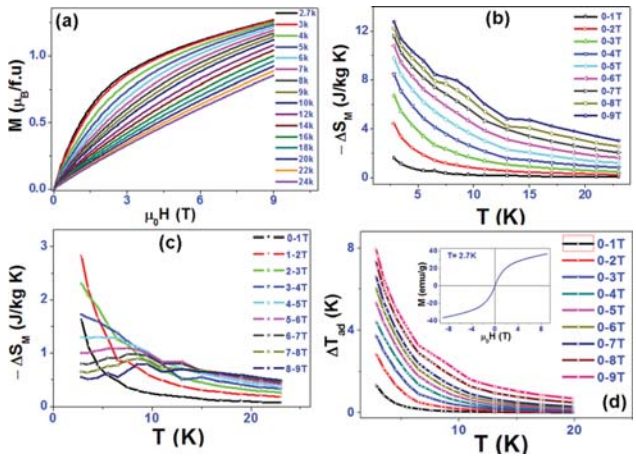

FIG. 3. (Color online) (a) *M-H* curves for $MnPS_3$ nanoparticles at temperatures from 2.7 K to 24 K. (b) $-\Delta S_M$ at temperatures from 2.85 K to 23 K for magnetic field changes from 0–1 T up to 0–9 T. (c) $-\Delta S_M$ at temperatures from 2.85 K to 23 K for magnetic field changes of 0–1, 1–2, 2–3, 3–4, 4–5, 5–6, 6–7, 7–8, and 8–9 T. (d) ΔT_{ad} at temperatures from 2.85 K to 23 K for magnetic field changes from 0–1 to 0–9 T, with a full *M-H* loop at 2.7 K presented in the inset.

the χ and C_P results. According to Ref. [20], the magnetic entropy change ($-\Delta S_M$) can be calculated as a function of temperature for magnetic field changes from 0–1 to 0–9 T, and the $-\Delta S_M$ results are displayed in Fig. 3(b). The curves present a characteristic shape with no peak over the entire temperature range, indicating that there is no transition and no long-range ordering of this electron/spin system. The magnitude of $-\Delta S_M$, at its maximum, increases with increasing magnetic field up to 4.5, 9.8, and 12.8 J/kg K at 2.85 K under fields of 2, 5, and 9 T, respectively. The magnetization hysteresis loop at 2.7 K (in Fig. 3(a)) indicates that there is no hysteresis loss and also indicates fully reversible behavior.

Because the heat capacity strongly depends on the external magnetic field, especially in the low temperature range,[20] in order to relatively precisely calculate $\Delta T_{ad}(T, H)$, we recalculated the $-\Delta S_M(T, \Delta H)$ ($\Delta H = 0$ to 1, 1 to 2,…, 8 to 9 T) for every magnetic field change of 1 T, and the results are shown in Fig. 3(c). We then calculated the $\Delta T_{ad}(T, \Delta H)$ according to Ref. [20], using the measured C_P data under relatively different external fields. The $\Delta T_{ad}(T, H)$ data under external field changes of 0 to H can then be obtained, as shown in Fig. 3(d). The maximum adiabatic temperature change (ΔT_{ad}) = 2.8, 5.3, and 8 K at 2.85 K for field changes of 2, 5, and 9 T, respectively. The $MnPS_3$ nanoparticles show very high ΔT_{ad}, which satisfies one of the important criteria for selecting magnetic refrigerants (i.e., a large adiabatic temperature change).

The values of $-\Delta S_M$ obtained for the $MnPS_3$ nanoparticle system are very large, with no magnetic/heat hysteresis, and the *M-H* loop at 2.7 K (as shown in the inset of Fig. 3(d)) indicates full reversibility. $-\Delta S_M$ is comparable with the values for any reported paramagnetic salts or nanosized garnets,[21] and for well designed molecular nanomagnets[22,23] for ultra-low temperature application, which exhibit second order or first order paramagnetic to ferromagnetic (or antiferromagnetic) phase transitions at a few degrees Kelvin. Furthermore, the $-\Delta S_M$ and ΔT_{ad} of the present material are higher than for those materials over the whole temperature range (2 to 20 K). These properties make $MnPS_3$ nanoparticles a promising candidate as a refrigerant at ultra-low temperatures.

The crystal structure of single crystal has been characterized very well[1]; the magnetic lattice has been modeled as Mn^{2+} honeycomb arranged antiferromagnetic interaction intra-planar and ferromagnetic coupling inter-planar with an angle of 107.35°.[2] The honeycomb lattice itself might exhibit a highly frustrated state and even an emergent spin-liquid state.[16,24] The restacked single layers cause distortions in the crystal structure[15] that might vary the spin vectors in the honeycomb spin lattice; give rise to highly frustrated spin states; and/or give rise to delocalized spins, free electrons, and competition due to interactions between these exotic states, leading to the emergence of abnormal magnetic properties.

In summary, microstructure analysis indicated that the nanoparticles were formed by the restacking of molecular layers that were stabilized via H_2O insertion between the layers. Long-range spin ordering, which exists in the bulk material, is canceled within the range of 2 K to 300 K. Susceptibility (χ) measurements and heat capacity results suggest the emergence of a low-lying energy spin state in this system. The actual MCE evaluation indicated that the system has a large reversible $-\Delta S_M$ of 6.8 and 12.8 J/kg K and ΔT_{ad} of 3.8 K and 8 K at 2.85 K for field changes of 3 T and 9 T, respectively, and $-\Delta S_m$ monotonically increases with decreasing temperature, which indicates that $MnPS_3$ in nanoparticle form is a potential candidate for application in magnetic refrigeration in the ultra-low-temperature range.

The authors thank Dr. T. Silver for her help and useful discussions. This work is supported by the Australian Research Council through a Discovery project (project ID: DP0879070).

[1]A. R. Wildes, H. M. Rønnow, *et al.*, Phys. Rev. B **74**, 094422 (2006); K. C. Rule, G. J. McIntyre, *et al.*, *ibid.* **76**, 134402 (2007).
[2]D. J. Goossens, A. J. Studer, *et al.*, J. Phys.: Condens. Matter **12**, 4233 (2000); K. C. Rule, A. R. Wildes, *et al.*, *ibid.* **21**, 124241 (2009); V. Grasso, F. Neri, *et al.*, Phys. Rev. B **42**, 1690 (1990); K. Kurosawa, S. Saito, and Y. Yamaguchi, J. Phys. Soc. Jpn. **52**, 3919 (1973).
[3]R. Brec, D. Schleigh, *et al.*, Inorg. Chem. **18**, 1814 (1979).
[4]P. A. Joy and S. Vasudevan, J. Am. Chem. Soc. **114**, 7792 (1992).
[5]P. G. Lacroix, R. Clement, *et al.*, Science **236**, 658 (1994).
[6]S. Yitzchaik, S. DiBella, *et al.*, J. Am. Chem. Soc. **19**, 2995 (1997).
[7]E. Delahaye, N. Sandeau, *et al.*, J. Phys. Chem. C **113**, 9092 (2009); Q. Liu, W. Zhou, *et al.*, Chem. Phys. Lett. **447**, 388 (2009).
[8]I. Lagadic, P. G. Lacroix, and R. Clement, Chem. Mater. **9**, 2004 (1997).
[9]A. Leaustic, E. Riviere, and R. Clement, Chem. Mater. **15**, 4784 (2003).
[10]M. Tokita, K. Zenmyo, *et al.*, J. Magn. Magn. Mater. **272–276**, 593 (2004).
[11]X. Zhang, X. Su, *et al.*, Synth. Met. **152**, 485 (2005); T. Masubuchi, H. Hoya, *et al.*, J. Alloys Compd. **460**, 668 (2007).
[12]D. Yang and R. F. Frindt, J. Mater. Res. **15**, 2408 (2000); A. A. El-Meligia *et al.*, J. Alloys Compd. **488**, 284 (2009).
[13]H. Falius, Z. Anorg. Allg. Chem. **356**, 189 (1968).
[14]R. F. Frindt, D. Yang, and P. Westreich, J. Mater. Res. **20**, 5 (2005).
[15]G. D. Du *et al.*, Chem. Commun. **46**, 1106 (2010).
[16]C. N. Varney, K. Sun, *et al.*, Phys. Rev. Lett. **107**, 077201 (2011).
[17]Y. Zhang and S. Das Sarma, Phys. Rev. Lett. **96**, 196602 (2006); J. Zhu and H. L. Stormer, *ibid.* **90**, 056805 (2003).
[18]D. Vollhardt, Rev. Mod. Phys. **56**, 99 (1984).
[19]K. G. Wilson, Rev. Mod. Phys. **47**, 773 (1975).
[20]A. M. Tishin, *The Magnetocaloric Effect and Its Applications* (Institute of Physics, Bristol, England, 2003).
[21]R. D. McMichael and R. D. Shull, J. Magn. Magn. Mater. **111**, 29 (1992).
[22]M. Manoli, A. Collins, *et al.*, J. Am. Chem. Soc. **130**, 11129 (2008).
[23]G. Karosis, M. Evanelisit, *et al.*, Angew. Chem., Int. Ed. **48**, 9928 (2009).
[24]Z. Y. Meng, T. C. Lang, *et al.*, Nature **464**, 847 (2010).

Downloaded 09 Oct 2012 to 130.130.37.84. Redistribution subject to AIP license or copyright; see http://jap.aip.org/about/rights_and_permissions